THE JOURNAL OF PHYSICAL CHEMISTRY C

Article

pubs.acs.org/JPCC

Stability of Chemically Passivated Silicon Electrodes in Aqueous Solutions: Interplay between Bias Voltage and Hydration of the Electrolyte

Vinicius R. Gonçales,[*,†] Yanfang Wu,[†] Bakul Gupta,[†,‡,§] Stephen G. Parker,[†,‡,§] Ying Yang,[†] Simone Ciampi,[∥] Richard Tilley,[†] and J. Justin Gooding[*,†,‡,§]

[†]School of Chemistry, [‡]Australian Centre for NanoMedicine, and [§]ARC Centre of Excellence in Convergent Bio-Nano Science and Technology, The University of New South Wales, Sydney, NSW 2052, Australia

[∥]Intelligent Polymer Research Institute, University of Wollongong, Wollongong, NSW 2522, Australia

Supporting Information

ABSTRACT: Chemical passivation of nonoxide semiconductors is a key prerequisite for electrochemical devices that operate in water-based electrolytes. Silicon remains the technologically most important material and organic monolayers based on the hydrosilylation of 1-alkynes have been shown to be a very effective approach to limit the thermodynamically favorable oxidation of the electrode, while still retaining efficient electron transfer across the solid/liquid interface. A large excess of a supporting electrolyte is always added to the solution in order to confine the applied potential gradient to the region close to the surface of the electrode. However, little is known about how the degree of solvation of the electrolyte species is linked to the degradation of the passivating chemistry. Here we test experimentally how electrolytes with different intrinsic hydration levels can influence the protection of the silicon as a function of surface biasing. X-ray photoelectron spectroscopy and contact angle experiments are used to determine under which conditions the chemical protection breaks down and oxidation of the silicon begins. Our results suggest that (i) anions seem to have a bigger impact on the growth of oxide than cations and (ii) the surface chemistry is more effective for protecting the semiconductor surface against oxidation in the presence of weakly hydrated ions. The utilization of strongly hydrated ions as the electrolyte dramatically diminishes the potential range in which the organic monolayer protects the silicon in aqueous environments.

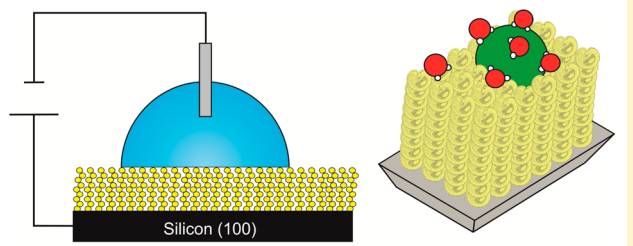

INTRODUCTION

The assembly of single-molecule-thick films on solid surfaces has been central to recent academic research, with notable examples including the preparation of sensors[1−3] and biomimetic interfaces[4,5] as well as the development of model laboratory systems to study subtle variables involved in electrode kinetics.[6,7] This methodology is of key importance to the electrochemical community, due to the precise control for incorporating chemical entities on the surface without blocking electron transfer across the solid/liquid interface. Examples in this field are reported on modifying noble and coinage metals using alkanethiol chemistry[8,9] and on functionalizing indium tin oxide (ITO) substrates with organophosphonic acid derivatives.[10,11] However, in recent years an area of considerable interest has been the modification of silicon surfaces with organic monolayers,[12−17] particularly the industrially relevant Si(100).[18−25]

The modification of Si(100), such that there is no intervening oxide layer, is both crucial and challenging to achieve.[26,27] A monolayer that prevents any oxygenated species reaching the Si(100) is particularly important as if this happens the Si(100) will oxidize. Such oxidation will alter the electronic properties of the device. The impact of ineffective monolayers was previously demonstrated on Si(100) electrodes used in aqueous solution where, upon scanning the electrode anodically, the silicon was observed to oxidize, and hence the electrode became passivated.[28] A promising surface chemistry strategy for protecting Si(100) from oxidation even when posed at positive potentials in aqueous media is to modify silicon with 1,8-nonadiyne, in which the strong terminal π-binding between the distal alkynes works to block penetration of H_2O and O_2 to the Si(100) surface. Although we have shown that 1000 anodic redox cycles could be performed without oxidizing the surface,[26] one unanswered question is what are the limits of the experimental conditions where an effective protection of Si(100) against the oxidation is maintained?

The purpose of this study is to begin to answer this question. The two main variables explored here are the electrolyte composition and the potential applied to the electrode. The

Special Issue: Kohei Uosaki Festschrift

Received: December 20, 2015
Published: February 2, 2016

DOI: 10.1021/acs.jpcc.5b12454
J. Phys. Chem. C 2016, 120, 15941−15948

impact of these variables was measured using X-ray photoelectron spectroscopy (XPS) and contact angle experiments to determine under which conditions the protection of the alkyne-terminated monolayer breaks down and oxidation of the Si(100) surface begins. The ionic species are varied according to the Hofmeister series because previous studies with alkanethiol-protected gold electrodes suggest that ionic permeability through the organic monolayers occurs at extreme potentials, both anodic and cathodic, which induces structural changes in the alkyl chains to accommodate the space-demanding ions and water molecules between them.[29−31] Although this effect was found to be reversible on alkanethiol-protected gold surfaces, this scenario may be more drastic for alkyne-terminated Si(100), as any water associated with a penetrating ion would be expected to promote surface oxidation, which would then deleteriously impact the electronic properties of the Si(100) electrode.

Generally, low charge density ions exhibit weaker interactions with water molecules than water itself. These ions have a lower probability of affecting the hydrogen bonding of the surrounding solvent, and they are named chaotropes. Otherwise, high charge density ions present stronger interactions with water molecules than water itself and therefore present higher probability of affecting the water structure. These ions are named kosmotropes. This denomination is linked to the observations performed by Hofmeister that different salts have distinct efficiencies at promoting salting-out of egg-white protein.[32] Previously, the conventional view was that competition between dissolved ions and dissolved proteins for hydration water would be responsible for this phenomenon. Nowadays, it is affirmed that more specific interactions between ions and proteins and ions and water molecules directly contacting the proteins may be a more important and contributing factor.[33] However, during the evolution of these studies, a ranking that parallels the Hofmeister series was developed for classifying the ions toward their properties for associating with water, as depicted in Table 1.

It was demonstrated previously that voltage and electrolyte pH can affect the kinetics of silicon oxidation.[35−40] However, for the specific case of silicon surfaces that are protected with organic monolayers the amount of water that the electrolyte ion can drag across the monolayer may become another variable linked to the anodic decomposition of the substrate. For this reason, it is evaluated in this article how the presence of chaotropic or kosmotropic ions in the electrolyte can affect the protection of the organic monolayers on Si(100) against surface oxidation as a function of surface bias. As the position of a given electrolyte in the Hofmeister series relates to its association with a water molecule, it is hypothesized that the breakdown of the protection of the silicon may depend on the nature of the electrolyte. The hypothesis is that, because at extremes of potentials ions will penetrate the organic monolayer[30,31] and will be able to reach the silicon surface, the more hydrated the ions in the electrolyte, the lower the protection of the Si(100) electrode by the organic monolayer. Understanding the rate of the passivation of silicon is important for developing electrochemical devices required to operate at distinct voltages in matrixes containing different electrolytes.

Table 1. Ions Employed in the Present Study as Electrolytes Are Depicted in the Table with the Respective $\Delta_{hyd}G$ Values, and Their Relative Position According to the Definition as Chaotropes (Present Weaker Interaction with Water Molecules than Water Itself) or Kosmotropes (Present Stronger Interaction with Water Molecules than Water Itself) Are Depicted in the Inset Figure

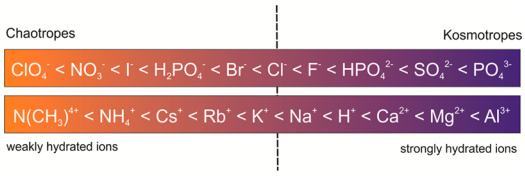

cations employed in this work	NH_4^+	Na^+	Mg^{2+}
theoretical $\Delta_{hyd}G$ (kJ mol^{-1})[34]	−285	−385	−1940
anions employed in this work	ClO_4^-	Cl^-	SO_4^{2-}
theoretical $\Delta_{hyd}G$ (kJ mol^{-1})[34]	−180	−270	−1145

EXPERIMENTAL METHODS

Chemicals. All chemicals were of analytical grade and used as received. Dichloromethane (DCM) and ethanol were distilled before use. Milli-Q water (~18 MΩ cm) was used for preparing solutions and for Si(100) cleaning procedures. Hydrogen peroxide (30 wt % in water, semiconductor grade, Sigma-Aldrich), hydrofluoric acid (Riedel-de Haën, 48 wt % in water), and sulfuric acid (semiconductor grade, Sigma-Aldrich) used for Si(100) cleaning and functionalization procedures were of high purity. 1,8-Nonadiyne (98%, Sigma) was distilled under reduced pressure from $NaBH_4$ (60 °C, 25−30 Torr) and stored under an ultrahigh purity argon atmosphere (O_2 < 5 ppb) prior to use. Prime-grade, p-type single-side polished Si wafers, 100-oriented (⟨100⟩ ± 0.5 °), 500−550 μm thick, 10−20 Ω cm resistivity were obtained from Siltronix Silicon Technologies (Archamps, France).

Assembly of Monolayers of 1,8-Nonadiyne on Si(100). Si(100) wafers were rinsed with DCM, dried under a stream of argon, and immersed in hot piranha solution (100 °C − 1 vol. 30 wt % H_2O_2/3 vol. H_2SO_4) for 1 h. Samples were then rinsed with a copious amount of Milli-Q water before being transferred to hydrofluoric acid (HF) aqueous solution (2.5 wt %) for 90 s. The HF treatment removed the native silica layer (SiO_x) and provided a hydrogen-terminated Si(100) surface. Hydrogen-terminated samples were immediately immersed into a degassed sample of 1,8-nonadiyne in order to form the alkyne-terminated Si(100) surface, as depicted in Scheme 1. The reaction flask was kept under argon atmosphere

Scheme 1. Covalent Attachment of 1,8-Nonadiyne on a Hydride-Terminated Si(100) Surface through Hydrosilylation Process[a]

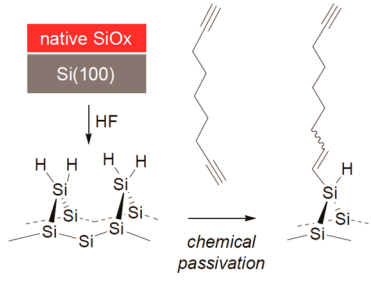

[a]The reaction was performed in the absence of H_2O and O_2 at 165 °C for 3 h. After this one-step procedure, an organic monolayer was built up on Si(100) with the triple bonds exposed onto the distal end.

DOI: 10.1021/acs.jpcc.5b12454
J. Phys. Chem. C 2016, 120, 15941−15948

and placed for 3 h in an oil bath set at 165 °C. After cooling to room temperature, the alkyne-terminated Si(100) surface was rinsed several times with DCM and rested in DCM at +4 °C under argon for 2 h. The alkyne-terminated Si(100) was then dried and kept under an argon atmosphere prior to use.

Experimental Measurements. Contact angle measurements were made on duplicated samples using a Ramé-Hart 200-F1 goniometer employing 6 μL of 4 M $NaClO_4$, 2 M $Mg(ClO_4)_2$, 4 M NH_4Cl, 4 M NaCl, 2 M $MgCl_2$, 2 M $(NH_4)_2SO_4$, 2 M Na_2SO_4, and 2 M $MgSO_4$ aqueous solutions. A WEP DC power supply PS-305D was employed for applying voltages using the alkyne-terminated Si(100) as the primary electrode and the stainless steel needle as the auxiliary electrode. The light intensity was fixed at 10.34 mW cm^{-2}. Ohmic contact to the silicon electrode was achieved by rubbing a Ga−In eutectic mixture onto the scratched backside of the Si(100) electrodes and pressing it against a copper plate. The contact angles were measured using the CorelDRAW X5 software at images recorded after 5 s of bias stimuli.

X-ray photoelectron spectroscopy (XPS) measurements were performed using an ESCALAB 220iXL spectrometer with a monochromatic Al Kα source (1486.6 eV). The pressure of the operating chamber was below 10^{-9} mbar, and spectra were recorded in normal emission. The spot diameter was 500 μm. The incidence angle was set to 58° to the analyzer lens. The resolution of the spectrometer is ca. 0.6 eV as measured from the Ag $3d_{5/2}$ signal (full width half-maximum) with 20 eV pass energy. Survey scans were carried out over 1300−0 eV range with a 1.0 eV step size, a 100 ms dwell time, and analyzer pass energy of 100 eV. High-resolution scans were run with 0.1 eV step size, dwell time of 100 ms, and analyzer pass energy set to 20 eV. The spectra were fitted with a convolution of Lorentzian and Gaussian profiles through Avantage software. The energies are termed as binding energies in eV and referenced to the C 1s signal (corrected to 284.8 eV).

RESULTS

Figure 1 illustrates the dependency of contact angle values with sample bias for 4 M NH_4Cl and 2 M $(NH_4)_2SO_4$. The average contact angle of a droplet of the ionic solutions was registered in function of the potential applied between the alkyne-terminated Si(100) and the stainless steel.

The static contact angle value was (88 ± 1)° at open circuit, which is in good agreement with previous literature.[26,27] When the alkyne-terminated Si(100) was scanned cathodically, the contact angle diminished quickly up to −1 V, achieving the values of (82 ± 2)° for 4 M NH_4Cl and (79 ± 1)° for 2 M NH_4SO_4 (Figure 1b). At −30 V, the contact angle was (71 ± 1)° for 4 M NH_4Cl, while it dropped significantly for the 2 M NH_4SO_4 system to (63 ± 1)° (Figure 1a). When the alkyne-terminated Si(100) was scanned anodically, the contact angle registered at +3.5 V was (73 ± 1)° for 4 M NH_4Cl and (67 ± 1)° for 2 M NH_4SO_4. When a voltage more positive than +3.5 V was applied at the alkyne-terminated Si(100), further spreading of the droplet was observed for both 4 M NH_4Cl and 2 M NH_4SO_4 (Figure 1a). This is attributed to the onset of oxidation of the silicon after this voltage, suggesting a significant breakdown in the protection of the surface by the organic film.

XPS profiles from Si 2p narrow scan were registered at the alkyne-terminated Si(100) after applying −30, −20, −10, +1, +2, and +3 V in the presence of 4 M NH_4Cl and 2 M NH_4SO_4. The results are illustrated in Figure 2.

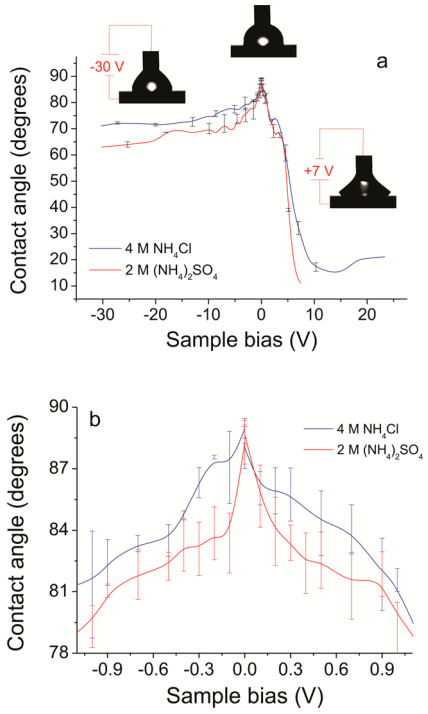

Figure 1. (a) Contact angle registered with a 6 μL droplet of (blue) 4 M NH_4Cl and (red) 2 M $(NH_4)SO_4$ by applying different voltages between the p-type (10−20 Ω cm) alkyne-terminated Si(100) surface and a stainless steel needle. Potential was applied under illumination using white light with energy above the bandgap value of Si (1.1 eV). The contact angle images presented as an inset in (a) are referred to the 4 M NH_4Cl solution. (b) Lower bias region (from −1 to +1 V) of the data shown in Figure 1a.

When the alkyne-terminated Si(100) was cathodically biased, no significant amount of SiO_x was formed in the presence of 4 M NH_4Cl solution up to −30 V (Figures 2b, 2c, and 2d). At these situations, the Si 2p narrow scan of the alkyne-terminated Si(100) revealed basically the $2p_{3/2}$ (99.2 eV) and $2p_{1/2}$ peaks (99.7 eV) characteristic of an oxide-free Si(100) surface. These profiles are similar to that obtained with the surface before it was biased at the different potentials (Figure 2a). This situation is surprisingly different from that observed when the alkyne-terminated Si(100) was probed in 2 M $(NH_4)_2SO_4$, where the appearance of a SiO_x peak at 102.1 eV was recognized at −20 V (Figure 2f) and −30 V (Figure 2g). When the alkyne-terminated Si(100) was anodically biased, formation of SiO_x occurred more easily in 2 M $(NH_4)_2SO_4$ relative to 4 M NH_4Cl. This is mainly noted by comparing the Si 2p narrow scan when the surface was biased at +1 V. Under these conditions, the Si 2p narrow scan obtained when the alkyne-terminated Si(100) was probed in 4 M NH_4Cl (Figure 2h) is typical of an oxide-free silicon surface. However, when the alkyne-terminated Si(100) was probed at +1 V in 2 M $(NH_4)_2SO_4$, a SiO_x peak was noted at 102.2 eV (Figure 2k).

The same series of experiments depicted in Figure 2 for 4 M NH_4Cl and 2 M $(NH_4)_2SO_4$ were repeated for 4 M $NaClO_4$, 2 M $Mg(ClO_4)_2$, 4 M NaCl, 2 M $MgCl_2$, 2 M Na_2SO_4, and 2 M $MgSO_4$ (Figures S1−S6 of the Supporting Information). The results were compared by plotting the oxide ratio [area of SiO_x peak/(area of SiO_x peak + area of Si $2p_{3/2}$ peak)]. This oxide ratio gives information about the percentage of SiO_x formed at different voltages when the alkyne-terminated Si(100) surface

DOI: 10.1021/acs.jpcc.5b12454
J. Phys. Chem. C 2016, 120, 15941−15948

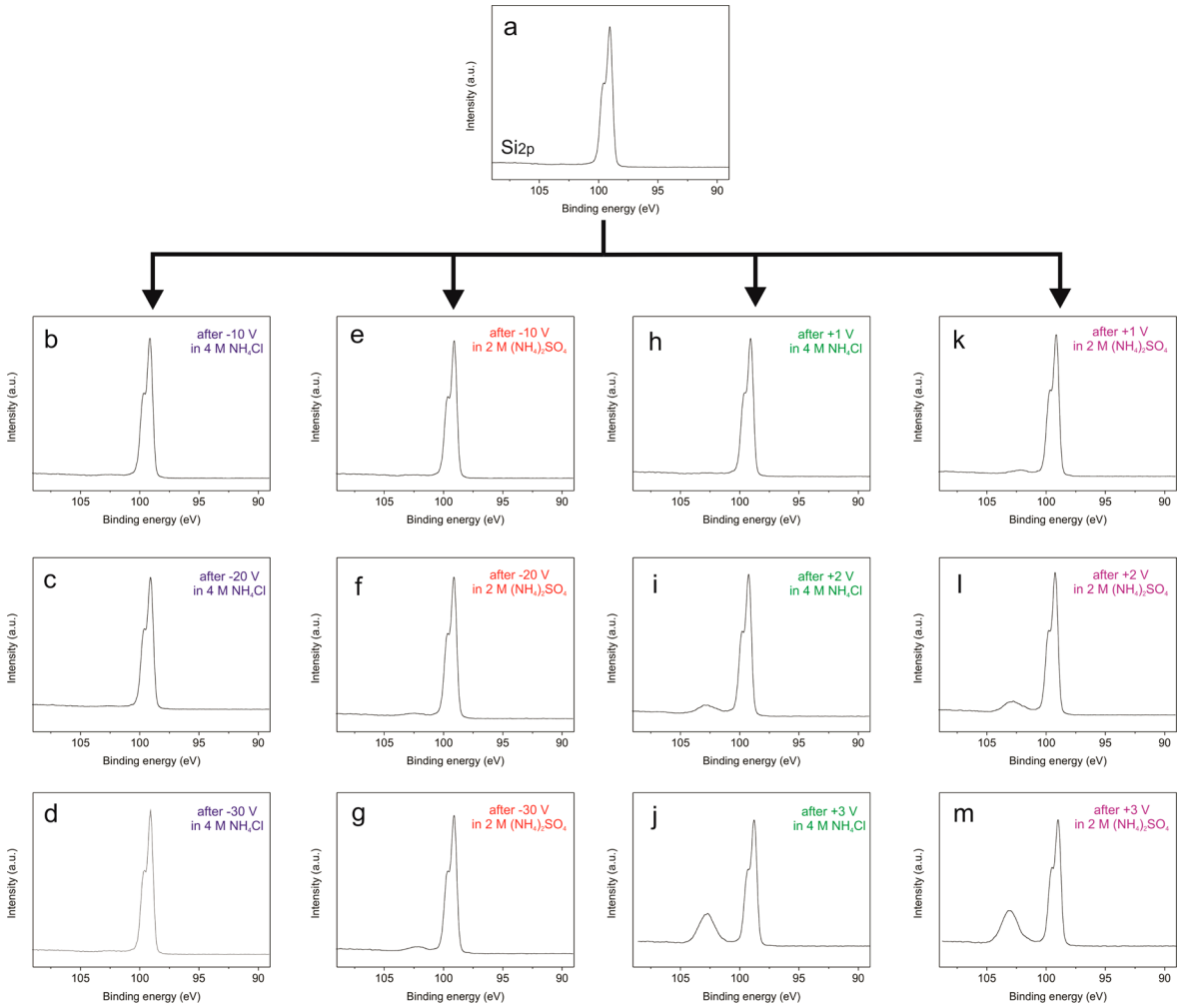

Figure 2. XPS data for Si 2p narrow scan on p-type (10−20 Ω cm) alkyne-terminated Si(100) (a) before and after applying (b) −10 V, (c) −20 V, and (d) −30 V using a 6 μL droplet of 4 M NH_4Cl as electrolyte; after applying (e) −10 V, (f) −20 V, and (g) −30 V using a 6 μL droplet of 2 M $(NH_4)_2SO_4$ as electrolyte; after applying (h) +1 V, (i) +2 V, and (j) +3 V using a 6 μL droplet of 4 M NH_4Cl as electrolyte; after applying (k) +1 V, (l) +2 V, and (m) +3 V using a 6 μL droplet of 4 M $(NH_4)_2SO_4$ as electrolyte. Potential was applied under top-side illumination using white light with energy above the bandgap value of Si (1.1 eV). The surfaces were biased for 5 s. Each entry is an independently prepared and analyzed surface.

was biased in the presence of the ionic solutions. The results are depicted in Table 2.

In order to compare the results depicted in Table 2, an arbitrary demarcation in the oxide ratios is made where below 0.020 surfaces are regarded as effectively protected by the organic monolayer during the electrochemical experiments. For example, the oxide ratio obtained after biasing the alkyne-terminated Si(100) at +1 V in 4 M NH_4Cl was 0.013, and a SiO_x peak cannot be easily discerned in Figure 2h. However, the oxide ratio obtained after biasing the alkyne-terminated Si(100) at +1 V in 2 M $(NH_4)_2SO_4$ was 0.052, and a SiO_x peak is easily visible in Figure 2k at 102.1 eV. This was also the case for the surfaces biased at +1 V in 2 M Na_2SO_4 (ratio = 0.043) and 2 M $MgSO_4$ (ratio = 0.091). When the alkyne-terminated Si(100) was cathodically biased using SO_4^{2-}-based solutions as electrolytes, an oxide ratio below 0.020 was achieved only at −10 V in 2 M $(NH_4)_2SO_4$ (ratio = 0.009). Oxide ratios above 0.020 were obtained when the surface was biased at −20 or −30 V in 2 M $(NH_4)_2SO_4$ or at any potential condition in 2 M Na_2SO_4 or 2 M $MgSO_4$. A SiO_x peak can be easily identified in the related XPS spectra (Figures S5 and S6 in Supporting Information).

Focusing our attention on the ClO_4^--based solutions, the oxide ratio obtained after biasing the alkyne-terminated Si(100) at +1 V in 4 M $NaClO_4$ was 0.006, and no significant SiO_x peak was observed at this condition. At the anodic direction, the protection of the organic monolayer against Si(100) oxidation was ineffective in 4 M $NaClO_4$ above +1 V, as noted by the oxide ratio 0.167 registered at +2 V. However, the oxide ratio obtained after biasing the alkyne-terminated Si(100) using 2 M $Mg(ClO_4)_2$ was already 0.050 at +1 V, indicating that the change of Na^+ for Mg^{2+} facilitated the formation of SiO_x. These results also suggest that changing SO_4^{2-} for ClO_4^--based solutions may affect the capability of the organic film to protect Si(100) against oxidation. This can also be noted when the alkyne-terminated Si(100) surface is cathodically biased. In that occasion, the obtained oxide ratios were below 0.020 for both 4 M $NaClO_4$ and 2 M $Mg(ClO_4)_2$. Indeed, the highest oxide ratio obtained was 0.012 when the alkyne-terminated Si(100) was biased at −20 V in 4 M $NaClO_4$. This value is significantly lower than the threshold of 0.020 postulated here, showing the efficiency of the alkyne monolayer on avoiding Si(100) oxidation at ClO_4^--based solutions. This was not the case for SO_4^{2-}-based solutions.

DOI: 10.1021/acs.jpcc.5b12454
J. Phys. Chem. C 2016, 120, 15941−15948

Table 2. Relative Comparison of the Amount of SiO_x Formed on the p-Type (10−20 Ω cm) Alkyne-Terminated Si(100) Surfaces after Applying −30, −20, −10, +1, and +2 V for 5 s Using a 6 μL Droplet of the Ionic Solution as Electrolyte[a]

[area of SiO_x peak/(area of SiO_x peak + area of Si $2p_{3/2}$ peak)]	-30 V	-20 V	-10 V	+1 V	+2 V
4 M $NaClO_4$	0.001	0.012	0.009	0.006	0.167
2 M $Mg(ClO_4)_2$	0.001	0.002	0.004	0.050	0.220
4 M NH_4Cl	0.013	0.006	0.012	0.013	0.137
4 M NaCl	0.012	0.013	0.019	0.007	0.115
2 M $MgCl_2$	0.014	0.012	0.012	0.040	0.242
2 M $(NH_4)_2SO_4$	0.076	0.040	0.009	0.052	0.184
2 M Na_2SO_4	0.047	0.081	0.061	0.043	0.211
2 M $MgSO_4$	0.053	0.042	0.042	0.091	0.209

[a]The oxide ratios are referred to [area of SiO_x peak/(area of SiO_x peak + area of Si $2p_{3/2}$ peak)]. The areas were calculated by fitting the Si 2p spectra with a convolution of Lorentzian and Gaussian profiles. During application of the potential, the surfaces were under top-side illumination using white light with energy above the bandgap value of Si (1.1 eV). Each entry is an independently prepared and analyzed surface.

Finally, the alkyne-terminated Si(100) was also biased in Cl^--based solutions. At +1 V, the obtained oxide ratios were 0.013 in 4 M NH_4Cl, 0.007 in 4 M NaCl, and 0.040 in 2 M $MgCl_2$. This means that the organic monolayer was more effective in avoiding Si(100) oxidation in 4 M NH_4Cl or 4 M NaCl than 2 M $MgCl_2$. When the alkyne-terminated Si(100) was biased at +2 V, the oxide ratios registered for all tested Cl^--based electrolytes were above 0.020, indicating significant oxidation of Si(100). When the alkyne-terminated surfaces were analyzed after being cathodically biased in Cl^--based solutions, the calculated oxide ratios were below 0.020 for all tested potentials and electrolytes. This means that the alkyne monolayer was effective on protecting the surface of significant oxidation, and no peaks could be observed on XPS without zooming the spectrum ∼102.5 eV. However, while the ClO_4^--based oxide ratios are basically located below 0.010, the Cl^--based oxide ratios are mainly situated between 0.010 and 0.020.

DISCUSSION

Contact angle measurements are a useful tool to inform about the macroscopic interaction of the aqueous solutions with the alkyne-terminated Si(100) surface to which a voltage is applied. When the surface was cathodically biased, the contact angle of a droplet of 4 M NH_4Cl diminished ∼7° up to −1 V, as illustrated in Figure 1b. The spreading can be understood in terms of the electrowetting phenomenon, that is, the electrical control of the wettability of liquids on a dielectric−(semi)-conductor system.[41−47] One should note though that the semiconductor employed in this work is a p-type Si(100) with doping level concentrations ∼10^{14} cm^{-3}. This means that under the depletion regime in the dark the space charge region is thick enough to make the semiconductor essentially behave as an insulating material, which would prevent the spreading of the droplet due to application of voltage. However, during the measurements the alkyne-terminated Si(100) is continuously illuminated using a light with energy above the bandgap value (1.1 eV). The illumination of the surface under this condition generates electron−hole pairs in the space-charge region, making the droplet respond similarly to the electrical stimulus as it does under the accumulation regime.[48] This phenomenon was demonstrated by Arscott using teflon−silicon systems, and it was referred to as photoelectrowetting.[49] A schematic representation of the phenomenon under the accumulation and depletion regimes is illustrated in Figure 3. The main

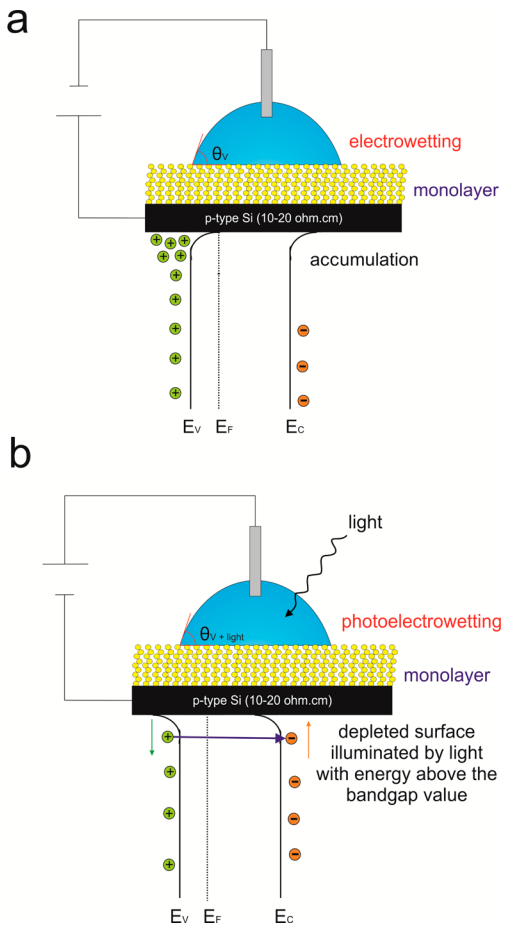

Figure 3. Illustrative cartoons demonstrating the droplet spreading at (a) the accumulation regime ($E > E_{flat\text{-}band}$), in which the system behaves as a liquid−dielectric−conductor platform and at (b) the depleted regime ($E < E_{flat\text{-}band}$) under illumination, in which electron−hole pairs are generated at the semiconductor-depleted zone, increasing the capacitance of the space-charge region and thus reducing the contact angle of the droplet at an applied potential.

difference is that here an organic monolayer with thickness of 10.4 Å[26] is employed as the dielectric material, instead of the Teflon-based polymers with thickness of 20 or 200 nm employed by Arscott. The main advantage of this approach is that a thin organic monolayer operating as the dielectric makes the spreading of the droplet possible at significantly lower voltages.[50] The main disadvantage is that the thinner layer can lead to a breakdown of the dielectric, making H_2O and ions penetrate through the organic monolayer and occasioning electrolysis between the liquid and electrode. It is intended here to explore this effect in the presence of different ions.

The profiles obtained during contact angle measurements as a function of potential were affected by using ionic solutions as electrolytes. The results obtained with 4 M NH_4Cl and 2 M $(NH_4)_2SO_4$ depicted in Figure 1 were chosen to illustrate the differences between electrolytes. When the alkyne-terminated surface was anodically scanned, the contact angle measure-

DOI: 10.1021/acs.jpcc.5b12454
J. Phys. Chem. C 2016, 120, 15941−15948

ments obtained up to +3.5 V with the 2 M $(NH_4)_2SO_4$ solution were slightly lower than the values registered with 4 M NH_4Cl. This effect was also noted when the alkyne-terminated Si(100) was cathodically biased, especially at potentials more negative than −1 V. This result is interesting because it initially suggests that the more strongly hydrated SO_4^{2-}-based systems respond to the electrostatic pressure[51] that originates for the applied potential causing the (photo)electrowetting effect, more effectively than less hydrated Cl^-. One should note though that contact angle measurements give information about the macroscopic interaction between solution and the surface, and understanding microscopically what is happening on the surface requires complementary analysis to correlate the registered spread with the formation or absence of SiO_x. The XPS spectra depicted in Figure 2 and the oxide ratios [area of SiO_x peak/(area of SiO_x peak + area of Si $2p_{3/2}$ peak)] calculated in Table 2 allow us to advance with this purpose.

When the alkyne-terminated Si(100) was anodically biased, oxide ratios above 0.020 were obtained at +2 V for the surface exposed to 4 M NH_4Cl and at +1 and +2 V for the surface exposed to 2 M $(NH_4)_2SO_4$. These values are less positive than the threshold potential of +3.5 V depicted in Figure 1, indicating that the larger spreading of the droplet is achieved only when the protection of the surface by the nonadiyne is already in an advanced stage of breakdown. The fact that the alkyne-terminated Si(100) is oxidized at potentials less positive in the presence of SO_4^{2-} than Cl^- was also an interesting observation. Although the presence of an organic monolayer reduces the interfacial capacitance from that associated with the bare surface, SO_4^{2-} and Cl^- anions accumulate at the distal end of the alkyne-terminated Si(100) when the surface is positively biased. It is speculated here that, since SO_4^{2-} is a more kosmotropic anion than Cl^-, the higher charge density could make it penetrate at lower voltages and drag a higher amount of water molecules through the organic monolayer. However, one should also note from Figure 2 and Table 2 that oxide ratios above 0.020 were obtained at −20 and −30 V for the surfaces exposed to 2 M $(NH_4)_2SO_4$, and oxide ratios below 0.020 were registered for the surfaces biased at −10, −20, and −30 V in the presence of 4 M NH_4Cl. The situation is not quite so straightforward, as the weakly hydrated NH_4^+ cations should accumulate at the distal end of the organic monolayer when the surface is negatively polarized. It is believed that ion pairing[52] might be responsible for this effect, which would cause occasional penetration of both hydrated cations and anions in the organic monolayer due to applied potential.

Similar conclusions were obtained by expanding the analysis for all the ionic solutions tested here. From Table 2, oxide ratios for SiO_x formation above 0.020 were obtained with SO_4^{2-}-based solutions at any tested potential, independently if the associated cations had a more a chaotropic or kosmotropic nature. The only exception was achieved when the alkyne-terminated Si(100) was biased at −10 V in 2 M $(NH_4)_2SO_4$, that is, in the presence of a weakly hydrated cation. The scenario changed when the alkyne-terminated Si(100) surfaces were biased in electrolytes containing the weakly hydrated ClO_4^- anions. In that case, oxide ratios above 0.020 were obtained at +1 V only if the system contained a strongly hydrated cation. When the surfaces were negatively biased, oxide ratios below 0.020 were obtained independently of whether the associated cations had a more chaotropic or kosmotropic nature. However, a comparison between the C 1s XPS narrow scan registered at the alkyne-terminated Si(100) samples after biased at −30 V in 4 M $NaClO_4$ and 2 M $Mg(ClO_4)_2$ is depicted in Figures 4b and 4c, respectively. Even

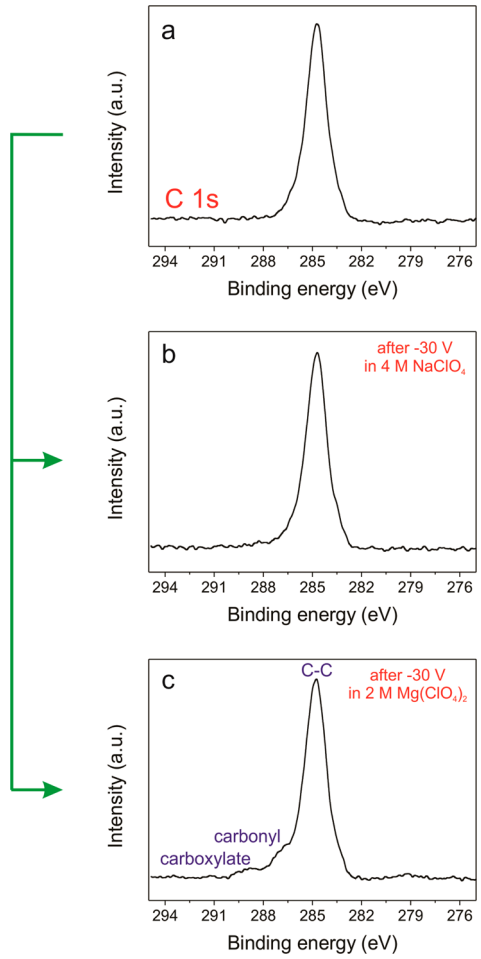

Figure 4. XPS data for C 1s narrow scan on p-type (10−20 Ω cm) alkyne-terminated Si(100) (a) before and after applying −30 V using a 6 μL droplet of (b) 4 M $NaClO_4$ and (c) 2 M $Mg(ClO_4)_2$ as electrolyte. Potential was applied under top-side illumination using white light with energy above the bandgap value of Si (1.1 eV).

though oxide ratios below 0.020 for SiO_x formations were obtained in both situations, the accumulation of the strongly hydrated Mg^{2+} cation in the Stern layer caused a greater change in the organic monolayer protection than the accumulation of Na^+, as revealed by the appearance of the carbonyl (287.0 eV) and carboxylic (289.0 eV) peaks.

CONCLUSION

Thus, it can be concluded that the different hydration of ions, for example as defined by the Hofmeister series, can govern the conditions under which the alkyne monolayer is able to protect a nonoxide semiconductor against anodic decomposition in aqueous electrolytes. For example, Cl^- anions bind to water molecules more strongly than ClO_4^- anions and more weakly than SO_4^{2-}, and our experimental results show that the monolayer-modified Si(100) surfaces exposed to Cl^--based electrolytes and biased at different voltages generally exhibit an oxide ratio usually higher than that obtained with the alkyne-terminated Si(100) surfaces biased in a ClO_4^--based electrolyte and lower than the oxide ratios obtained with the surfaces tested in SO_4^{2-}-based electrolytes. One should note though

DOI: 10.1021/acs.jpcc.5b12454
J. Phys. Chem. C 2016, 120, 15941−15948

that the presence of a strongly hydrated cation may affect this relation. For example, the oxide ratio for SiO_x formation for the surfaces biased at +1 V in 2 M $Mg(ClO_4)_2$ are higher than the values obtained with the alkyne-terminated surfaces biased at +1 V in 4 M NH_4Cl or 4 M NaCl.

The data presented herein provide some guidelines for the use of electrolytes if using monolayer-modified silicon surfaces for the protection against oxidation. To identify these trends first requires that the data for the alkyne-terminated surface biased at +2 V be disregarded. The justification for this is the extent of oxidation is such that the organic monolayer is significantly compromised in all the tested cases. With this in mind the trends that emerge from the data suggest that anions seem to have a bigger impact on the growth of oxide than cations. Second, contrary to expectations, ions with the same charge as the potential applied to the surface have more of an effect than the oppositely charged ions. Finally, as expected the more kosmotropic, more hydrated ions lead to more oxidation of the silicon than the weakly chaotropic ions. With these trends in mind, given the choice, perchlorate would be the best anion for protection of the silicon, while sulfate and highly kosmotropic cations should be avoided. These results will enable researchers to design more robust electrochemical devices based on silicon through the careful choice of the supporting electrolyte.

■ ASSOCIATED CONTENT

Supporting Information

The Supporting Information is available free of charge on the ACS Publications website at DOI: 10.1021/acs.jpcc.5b12454.

XPS data for Si 2p narrow scan on p-type (10−20 Ω cm) alkyne-terminated Si(100) after applying −30, −20, −10, +1, +2, and +3 V using a 6 μL droplet of 4 M $NaClO_4$, 2 M $Mg(ClO_4)_2$, 4 M NaCl, 2 M $MgCl_2$, 2 M Na_2SO_4, and 2 M $MgSO_4$ as electrolyte (PDF)

■ AUTHOR INFORMATION

Corresponding Authors

*E-mail: v.goncales@unsw.edu.au.

*E-mail: justin.gooding@unsw.edu.au.

Notes

The authors declare no competing financial interest.

■ ACKNOWLEDGMENTS

V.R.G. thanks CAPES-Brazil (Proc. 12149-13-6) for the conceded scholarship. This research was supported by the Australian Research Council (ARC) under the Discovery Projects Funding Scheme (DP150103065) and by the ARC Centre of Excellence for Convergent Bio-Nano Science and Technology (CE140100036).

■ REFERENCES

(1) Gupta, B.; Mai, K.; Lowe, S. B.; Wakefield, D.; Di Girolamo, N.; Gaus, K.; Reece, P. J.; Gooding, J. J. Ultrasensitive and Specific Measurement of Protease Activity Using Functionalized Photonic Crystals. *Anal. Chem.* **2015**, *87*, 9946−9953.

(2) Suherman; Morita, K.; Kawaguchi, T. Effect of Alkanethiol Molecular Structure on Sensitivity of Surface Plasmon Resonance Sensor. *Sens. Actuators, B* **2015**, *210*, 768−775.

(3) Tavallaie, R.; Darwish, N.; Gebala, M.; Hibbert, D. B.; Gooding, J. J. The Effect of Interfacial Design on the Electrochemical Detection of DNA and Microrna Using Methylene Blue at Low-Density DNA Films. *ChemElectroChem* **2014**, *1*, 165−171.

(4) Ng, C. C. A.; Magenau, A.; Ngalim, S. H.; Ciampi, S.; Chockalingham, M.; Harper, J. B.; Gaus, K.; Gooding, J. J. Using an Electrical Potential to Reversibly Switch Surfaces between Two States for Dynamically Controlling Cell Adhesion. *Angew. Chem., Int. Ed.* **2012**, *51*, 7706−7710.

(5) Sobers, C. J.; Wood, S. E.; Mrksich, M. A Gene Expression-Based Comparison of Cell Adhesion to Extracellular Matrix and Rgd-Terminated Monolayers. *Biomaterials* **2015**, *52*, 385−394.

(6) Ciampi, S.; Choudhury, M. H.; Ahmad, S. A. B. A.; Darwish, N.; Brun, A. L.; Gooding, J. J. The Impact of Surface Coverage on the Kinetics of Electron Transfer through Redox Monolayers on a Silicon Electrode Surface. *Electrochim. Acta* **2015**, *186*, 216−222.

(7) Fabre, B. Ferrocene-Terminated Monolayers Covalently Bound to Hydrogen-Terminated Silicon Surfaces. Toward the Development of Charge Storage and Communication Devices. *Acc. Chem. Res.* **2010**, *43*, 1509−1518.

(8) Love, J. C.; Estroff, L. a.; Kriebel, J. K.; Nuzzo, R. G.; Whitesides, G. M. Self-Assembled Monolayers of Thiolates on Metals as a Form of Nanotechnology. *Chem. Rev.* **2005**, *105*, 1103−1170.

(9) Vericat, C.; Vela, M. E.; Benitez, G.; Carro, P.; Salvarezza, R. C. Self-Assembled Monolayers of Thiols and Dithiols on Gold: New Challenges for a Well-Known System. *Chem. Soc. Rev.* **2010**, *39*, 1805−1834.

(10) Chockalingam, M.; Darwish, N.; Le Saux, G.; Gooding, J. J. Importance of the Indium Tin Oxide Substrate on the Quality of Self-Assembled Monolayers Formed from Organophosphonic Acids. *Langmuir* **2011**, *27*, 2545−2552.

(11) Chockalingam, M.; Magenau, A.; Parker, S. G.; Parviz, M.; Vivekchand, S. R. C.; Gaus, K.; Gooding, J. J. Biointerfaces on Indium−Tin Oxide Prepared from Organophosphonic Acid Self-Assembled Monolayers. *Langmuir* **2014**, *30*, 8509−8515.

(12) Fabre, B.; Hauquier, F. Single-Component and Mixed Ferrocene-Terminated Alkyl Monolayers Covalently Bound to Si(111) Surfaces. *J. Phys. Chem. B* **2006**, *110*, 6848−6855.

(13) Fabre, B.; Lopinski, G. P.; Wayner, D. D. M. Functionalization of Si(111) Surfaces with Alkyl Chains Terminated by Electrochemically Polymerizable Thienyl Units. *Chem. Commun. (Cambridge, U. K.)* **2002**, *5*, 2904−2905.

(14) Fabre, B.; Lopinski, G. P.; Wayner, D. D. M. Photoelectrochemical Generation of Electronically Conducting Polymer-Based Hybrid Junctions on Modified Si(111) Surfaces. *J. Phys. Chem. B* **2003**, *107*, 14326−14335.

(15) Fabre, B.; Pujari, S. P.; Scheres, L.; Zuilhof, H. Micropatterned Ferrocenyl Monolayers Covalently Bound to Hydrogen-Terminated Silicon Surfaces: Effects of Pattern Size on the Cyclic Voltammetry and Capacitance Characteristics. *Langmuir* **2014**, *30*, 7235−7243.

(16) Linford, M. R.; Fenter, P.; Eisenberger, P. M.; Chidsey, C. E. D. Alkyl Monolayers on Silicon Prepared from 1-Alkenes and Hydrogen-Terminated Silicon. *J. Am. Chem. Soc.* **1995**, *117*, 3145−3155.

(17) Rohde, R. D.; Agnew, H. D.; Yeo, W.-S.; Bailey, R. C.; Heath, J. R. A Non-Oxidative Approach toward Chemically and Electrochemically Functionalizing Si(111). *J. Am. Chem. Soc.* **2006**, *128*, 9518−9525.

(18) Ciampi, S.; Harper, J. B.; Gooding, J. J. Wet Chemical Routes to the Assembly of Organic Monolayers on Silicon Surfaces Via the Formation of Si-C Bonds: Surface Preparation, Passivation and Functionalization. *Chem. Soc. Rev.* **2010**, *39*, 2158−2183.

(19) Decker, F.; Cattaruzza, F.; Coluzza, C.; Flamini, A.; Marrani, A. G.; Zanoni, R.; Dalchiele, E. A. Electrochemical Reversibility of Vinylferrocene Monolayers Covalently Attached on H-Terminated P-Si(100). *J. Phys. Chem. B* **2006**, *110*, 7374−7379.

(20) Linford, M. R.; Chidsey, C. E. D. Alkyl Monolayers Covalently Bonded to Silicon Surfaces. *J. Am. Chem. Soc.* **1993**, *115*, 12631−12632.

(21) Marrani, A. G.; Cattaruzza, F.; Decker, F.; Galloni, P.; Zanoni, R. Chemical Routes to Fine Tuning the Redox Potential of Monolayers Covalently Attached on H−Si(100). *Electrochim. Acta* **2010**, *55*, 5733−5740.

DOI: 10.1021/acs.jpcc.5b12454
J. Phys. Chem. C 2016, 120, 15941−15948

(22) Sieval, a. B.; Demirel, a. L.; Nissink, J. W. M.; Linford, M. R.; Maas, J. H. V. D.; Jeu, W. H. D.; Zuilhof, H.; Sudhölter, E. J. R. Highly Stable Si-C Linked Functionalized Monolayers on the Silicon (100) Surface. *Langmuir* **1998**, *14*, 1759−1768.
(23) Sung, M. M.; Kluth, G. J.; Yauw, O. W.; Maboudian, R. Thermal Behavior of Alkyl Monolayers on Silicon Surfaces. *Langmuir* **1997**, *13*, 6164−6168.
(24) Zanoni, R.; Aurora, A.; Cattaruzza, F.; Coluzza, C.; Dalchiele, E. A.; Decker, F.; Di Santo, G.; Flamini, A.; Funari, L.; Marrani, A. G. A Mild Functionalization Route to Robust Molecular Electroactive Monolayers on Si(100). *Mater. Sci. Eng., C* **2006**, *26*, 840−845.
(25) Zanoni, R.; Cattaruzza, F.; Coluzza, C.; Dalchiele, E. A.; Decker, F.; Di Santo, G.; Flamini, A.; Funari, L.; Marrani, A. G. An Afm, Xps and Electrochemical Study of Molecular Electroactive Monolayers Formed by Wet Chemistry Functionalization of H-Terminated Si(100) with Vinylferrocene. *Surf. Sci.* **2005**, *575*, 260−272.
(26) Ciampi, S.; Eggers, P. K.; Le Saux, G.; James, M.; Harper, J. B.; Gooding, J. J. Silicon (100) Electrodes Resistant to Oxidation in Aqueous Solutions: An Unexpected Benefit of Surface Acetylene Moieties. *Langmuir* **2009**, *25*, 2530−2539.
(27) Ng, A.; Ciampi, S.; James, M.; Harper, J. B.; Gooding, J. J. Comparing the Reactivity of Alkynes and Alkenes on Silicon (100) Surfaces. *Langmuir* **2009**, *25*, 13934−41.
(28) Yu, J. X.; Losic, D.; Marshall, M.; Bocking, T.; Gooding, J. J.; Shapter, J. G. Preparation and Characterisation of an Aligned Carbon Nanotube Array on the Silicon (100) Surface. *Soft Matter* **2006**, *2*, 1081−1088.
(29) Björefors, F.; Petoral, R. M.; Uvdal, K. Electrochemical Impedance Spectroscopy for Investigations on Ion Permeation in Ω-Functionalized Self-Assembled Monolayers. *Anal. Chem.* **2007**, *79*, 8391−8398.
(30) Darwish, N.; Eggers, P. K.; Ciampi, S.; Zhang, Y.; Tong, Y.; Ye, S.; Paddon-Row, M. N.; Gooding, J. J. Reversible Potential-Induced Structural Changes of Alkanethiol Monolayers on Gold Surfaces. *Electrochem. Commun.* **2011**, *13*, 387−390.
(31) Góes, M. S.; Rahman, H.; Ryall, J.; Davis, J. J.; Bueno, P. R. A Dielectric Model of Self-Assembled Monolayer Interfaces by Capacitive Spectroscopy†. *Langmuir* **2012**, *28*, 9689−9699.
(32) Kunz, W.; Henle, J.; Ninham, B. W. 'Zur Lehre Von Der Wirkung Der Salze' (About the Science of the Effect of Salts): Franz Hofmeister's Historical Papers. *Curr. Opin. Colloid Interface Sci.* **2004**, *9*, 19−37.
(33) Zhang, Y.; Cremer, P. S. Interactions between Macromolecules and Ions: The Hofmeister Series. *Curr. Opin. Chem. Biol.* **2006**, *10*, 658−63.
(34) Marcus, Y. Thermodynamics of Solvation of Ions. *J. Chem. Soc., Faraday Trans.* **1991**, *87*, 2995−2999.
(35) Avouris, P.; Hertel, T.; Martel, R. Atomic Force Microscope Tip-Induced Local Oxidation of Silicon: Kinetics, Mechanism, and Nanofabrication. *Appl. Phys. Lett.* **1997**, *71*, 285−287.
(36) Avouris, P.; Martel, R.; Hertel, T.; Sandstrom, R. Afm-Tip-Induced and Current-Induced Local Oxidation of Silicon Andmetals. *Appl. Phys. A: Mater. Sci. Process.* **1998**, *66*, 659−667.
(37) Gerischer, H.; Allongue, P.; Costa Kieling, V. The Mechanism of the Anodic Oxidation of Silicon in Acidic Fluoride Solutions Revisited. *Berichte der Bunsengesellschaft für physikalische Chemie* **1993**, *97*, 753−757.
(38) Gerischer, H.; Lübke, M. The Electrochemical Behaviour of N-Type Silicon (111)-Surfaces in Fluoride Containing Aqueous Electrolytes. *Berichte der Bunsengesellschaft für Physikalische Chemie* **1987**, *91*, 394−398.
(39) Genscher, H.; Lübke, M. Electrolytic Growth and Dissolution of Oxide Layers on Silicon in Aqueous Solutions of Fluorides. *Ber. Bunsenges. Phys. Chem.* **1988**, *92*, 573−577.
(40) Schmidt, P. F.; Michel, W. Anodic Formation of Oxide Films on Silicon. *J. Electrochem. Soc.* **1957**, *104*, 230−236.
(41) Cho, S. K.; Moon, H.; Kim, C.-J. Creating, Transporting, Cutting, and Merging Liquid Droplets by Electrowetting-Based Actuation for Digital Microfluidic Circuits. *J. Microelectromech. Syst.* **2003**, *12*, 70−80.
(42) Liu, H.; Dharmatilleke, S.; Maurya, D. K.; Tay, A. a. O. Dielectric Materials for Electrowetting-on-Dielectric Actuation. *Microsyst. Technol.* **2010**, *16*, 449−460.
(43) Lapierre, F.; Coffinier, Y.; Boukherroub, R.; Thomy, V. Electro-(De)Wetting on Superhydrophobic Surfaces. *Langmuir* **2013**, *29*, 13346−51.
(44) Lee, J.; Moon, H.; Fowler, J.; Schoellhammer, T.; Kim, C.-J. Electrowetting and Electrowetting-on-Dielectric for Microscale Liquid Handling. *Sens. Actuators, A* **2002**, *95*, 259−268.
(45) Rajkumar, K.; Rajendrakumar, R. T. Fabrication and Electrowetting Properties of Poly Si Nanostructure Based Superhydrophobic Platform. *Plasma Chem. Plasma Process.* **2013**, *33*, 807−816.
(46) Narasimhan, V.; Park, S.-Y. An Ion Gel as a Low-Cost, Spin-Coatable, High-Capacitance Dielectric for Electrowetting-on-Dielectric (Ewod). *Langmuir* **2015**, *31*, 8512−8518.
(47) Zhang, X.; Di, Q.; Zhu, F.; Sun, G.; Zhang, H. Superhydrophobic Micro/Nano Dual-Scale Structures. *J. Nanosci. Nanotechnol.* **2013**, *13*, 1539−1542.
(48) Choudhury, M. H.; Ciampi, S.; Yang, Y.; Tavallaie, R.; Zhu, Y.; Zarei, L.; Gonçales, V. R.; Gooding, J. J. Connecting Electrodes with Light: One Wire, Many Electrodes. *Chem. Sci.* **2015**, *6*, 6769−6776.
(49) Arscott, S. Moving Liquids with Light: Photoelectrowetting on Semiconductors. *Sci. Rep.* **2011**, *1*, 184.
(50) Chang, Y.-W.; Kwok, D. Y. Electrowetting on Dielectric: A Low Voltage Study on Self-Assembled Monolayers and Its Wetting Kinetics. In *2004 International Conference on MEMS, NANO and Smart Systems (ICMENS'04)*, IEEE: 2004; pp 66−71.
(51) Kang, K. H. How Electrostatic Fields Change Contact Angle in Electrowetting. *Langmuir* **2002**, *18*, 10318−10322.
(52) Chen, H.; Ruckenstein, E. Hydrated Ions: From Individual Ions to Ion Pairs to Ion Clusters. *J. Phys. Chem. B* **2015**, *119*, 12671−12676.

DOI: 10.1021/acs.jpcc.5b12454
J. Phys. Chem. C 2016, 120, 15941−15948